1A.3 LARGE-EDDY SIMULATION OF A STRATOCUMULUS TO CUMULUS CLOUD TRANSITION AS OBSERVED DURING ASTEX

Stephan R. de ROODE[*] and Johan van der DUSSEN

Multi-Scale Physics, Delft University of Technology, The Netherlands

ABSTRACT

Large-eddy simulation (LES) results of the First Lagrangian during the Atlantic Stratocumulus Transition EXperiment (ASTEX) are compared with aircraft observations. In this experiment a column of air was tracked for 48 hours as it moved south-westward over water with increasing sea surface temperatures. A key feature of the boundary layer evolution is a gradual weakening of the inversion stability. The cloud developed from a solid well-mixed stratocumulus layer to a layer filled with cumulus clouds penetrating thin and broken stratocumulus above. The model was initialized identically to a previous GCSS model intercomparison case based on the second aircraft flight A209. The Dutch Atmospheric LES (DALES) model includes a two-moment scheme for drizzle. It is found from the LES results that drizzle and cloud droplet sedimentation tend to diminish the entrainment rate. Furthermore radiative transfer for both the shortwave and longwave bands is calculated for the full atmospheric column. Because ERA-interim results for the divergence differ from ERA-40, two simulations with different large-scale divergence rates are performed. In the simulation with a constant divergence rate $D = 5 \times 10^{-6}$ s^{-1} the boundary layer grows slower than the one in which the divergence rate gradually becomes slightly negative ($D = -1 \times 10^{-6}$ s^{-1}). The difference in the boundary layer height is partly due to the fact that a more positive divergence rate causes a stronger large-scale subsidence velocity that pushes down the boundary layer top faster. In addition, the large-scale subsidence determines the tendencies of heat and moisture above the boundary layer depth, which, in turn, affect the inversion stability. A more stable inversion stratification diminishes the entrainment rate. The observations showed a significant increase of turbulence during the second night, which is well represented by the LES model for both simulations. Additional LES results will be collected and compared to the results as part of the EUCLIPSE/GCSS ASTEX model intercomparison study.

1. INTRODUCTION

The presence of a strong thermal inversion in the subtropical part of the Hadley circulation efficiently traps the moisture that is evaporated from the ocean. As a result extended stratocumulus cloud fields persist in these areas. This cloudy air is transported equatorwards over increasingly higher sea surface temperatures by the trade-winds, and stratocumulus is gradually replaced by shallow cumulus. The latter cloud type has a lower cloud fraction, allowing a much higher fraction of the downwelling shortwave radiation to reach the sea surface. It is therefore important for weather and climate models to realistically represent this cloud regime.

Sandu et al. (2010) analysed satellite data to determine trajectories of airmasses in which a transition from stratocumulus to cumulus takes place. Based on the results, composite model intercomparison cases of a fast and of a relatively slow transition were set up. The results show that the sea surface temperature, which largely determines the inversion strength, plays a crucial role in the pace of the transition (Sandu and Stevens, 2010).

The Atlantic Stratocumulus Transition EXperiment (ASTEX) was set up in order to characterise the evolution and vertical structure of a marine boundary layer (Albrecht et al., 1995). In ASTEX a very successful experiment was carried out during the "First Lagrangian", in which an air mass was followed for two days between 12 and 14 June 1992.
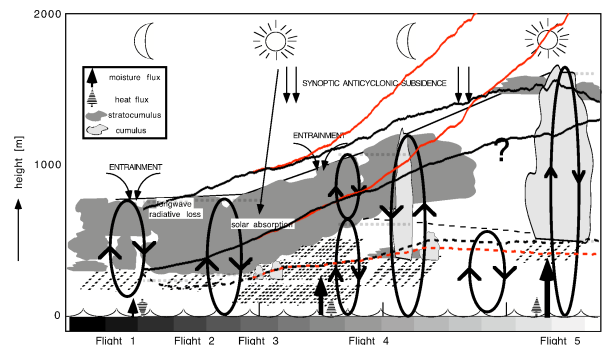

FIG. 1: Schematic of the observed Lagrangian transition from five aircraft flights during the first ASTEX Lagrangian. The thick lines indicate LES results for the domain averaged cloud top and base (solid lines) and the minimum cloud base (dashed lines) for two different time series for the large-scale divergence rate (constant for the black lines and becoming slightly negative for the red lines.

Figure 1 shows schematically the evolution of the cloud deck in this air mass, as it was advected by the mean wind over an increasing sea surface temperature. As a result, a solid stratocumulus deck gradually dissipated into thin and broken patches, which were penetrated from below by cumulus clouds (De Roode and Duynkerke, 1996). The cloud transition was observed from five consecutive aircraft flights from which the evo-

---

[*] *Corresponding author address:* Stephan de Roode, Dept. of Multi-Scale Physics, Delft University of Technology, Delft, The Netherlands (s.r.deroode@tudelft.nl - www.msp.tudelft.nl)

lution of the mean state and turbulence structure of the boundary layer could be analysed (Bretherton et al., 1995; De Roode and Duynkerke, 1997).

The second (Duynkerke et al., 1995) and third (Duynkerke et al., 1999) flights of the ASTEX Lagrangian, both being nighttime cases, have been used for two LES model intercomparison studies[1,2]. Due to limited computational resources, the simulations lasted only three hours. The main emphasis was on the comparison of the entrainment rate and the turbulence structure between the models and the observations.

Bretherton et al. (1999a) presented results of simulations of the First Lagrangian obtained with single-column model versions of large-scale models. The models all predicted the observed deepening and decoupling of the boundary layer quite well, with cumulus cloud evolution and thinning of the overlying stratocumulus. The models also produced realistic drizzle rates, but there were substantial quantitative differences in the cloud cover and liquid water path between models. Van der Dussen (2001) found a good agreement between the observations and results from large-eddy simulations of the ASTEX Lagrangian which used simple parameterizations for longwave (Stevens et al., 2005) and shortwave (Duynkerke et al., 2004) radiation.

The strong increase in computational power now allows for studying the full transition with a new generation large-eddy simulation models. Major improvements to these models in the last decade include the incorporation of detailed shortwave and longwave radiation schemes (Pincus and Stevens, 2009) and modules for drizzle (Khairoutdinov and Kogan, 2000; Seifert and Beheng, 2001).

This paper presents some preliminary results of large-eddy simulations that are part of a revised ASTEX Lagrangian model intercomparison case. The main question asked is to what extent LES models can reproduce the observed evolution of the mean state and turbulence structure in the boundary layer, caused by the increase of the sea surface temperature and the large-scale subsidence.

2. SET UP

2.1 *Initial conditions*

The simulations start at 13 June 00 UTC, and the initial vertical profiles of the liquid water potential temperature (θ_L), total humidity (q_T), and the east-west and north-south wind velocities (u and v, respectively) are taken identical to the set-up originally proposed for the GCSS ASTEX A209 case.

The base of the entrainment zone is initially at a height of $z_i = 662.5$ m. Below, the boundary layer is assumed to be well mixed. Therefore, the initial profiles

---

[1] http://www.phys.uu.nl/~wwwimau/old/ASTEX/astexcomp.html
[2] http://www.phys.uu.nl/~wwwimau/old/EUCREM/eucrem.html

---

for $0 < z \leq z_i$ read:

$$
\begin{aligned}
u &= -0.7 && (\mathrm{ms}^{-1}) \\
v &= -10.0 && (\mathrm{ms}^{-1}) \\
\theta_L &= 288 && (\mathrm{K}) \\
q_T &= 10.2 && (\mathrm{g\,kg}^{-1})
\end{aligned}
$$

The inversion layer has a thickness of $\Delta z_i = 50$ m. Inside it (for $z_i < z \leq z_i + \Delta z_i$) the profiles are as follows:

$$
\begin{aligned}
u &= -0.7 - 0.026\,(z - z_i) && (\mathrm{ms}^{-1}) \\
v &= -10.0 && (\mathrm{ms}^{-1}) \\
\theta_L &= 288 + \Delta\theta_L(z - z_i)/\Delta z_i && (\mathrm{K}) \\
q_T &= 10.2 + \Delta q_T(z - z_i)/\Delta z_i && (\mathrm{g\,kg}^{-1})
\end{aligned}
$$

in which the initial inversion jumps $\Delta\theta_L$ and Δq_T are 5.5 K and -1.1 g kg^{-1} respectively. In the free atmosphere (for $z > z_i + \Delta z_i$), the profiles of q_T and θ_L are determined by the free atmospheric lapse rates $\Gamma_\theta = (\partial\theta_L/\partial z)_{FA} = 6$ K km and $\Gamma_q = (\partial q_T/\partial z)_{FA} = -2.8$ g kg^{-1} km^{-1}, according to:

$$
\begin{aligned}
u &= -2.0 && (\mathrm{ms}^{-1}) \\
v &= -10.0 && (\mathrm{ms}^{-1}) \\
\theta_L &= 288 + \Delta\theta_L + \Gamma_\theta(z - z_i - \Delta z_i) && (\mathrm{K}) \\
q_T &= 10.2 + \Delta q_T + \Gamma_q(z - z_i - \Delta z_i) && (\mathrm{g\,kg}^{-1})
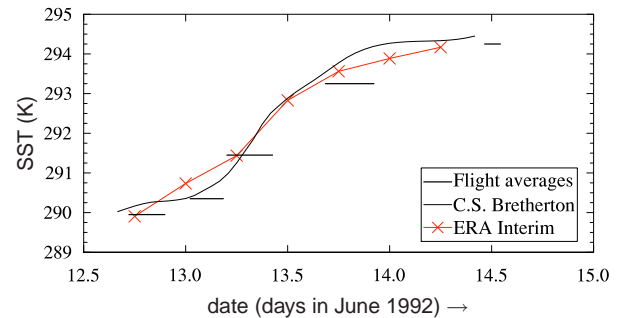\end{aligned}
$$

FIG. 2: The sea surface temperature as a function of time during the first Lagrangian, as provided by C.S. Bretherton (black line) and as found in the ERA Interim data (red line). The horizontal black lines show the times of the different flight legs and the mean SST during these flights. The uncertainty in these measurements is of the order of 0.5 K (De Roode and Duynkerke, 1997).

2.2 *Boundary conditions and model forcing*

For the full radiation scheme it is required to prescribe the vertical thermodynamical structure of the atmosphere above the LES domain. Data from the ERA-Interim reanalysis project was used to approximate the temperature, the water vapor content and the amount of ozon, during the transition, up to a height of 1 hPa.

The sea surface temperature used, is taken from the dataset compiled by Chris Bretherton[3], which compares quite well with the measurements in the first half of the transition (see Fig. 2), while in the second part, the ERA Interim data is closer to the observations.
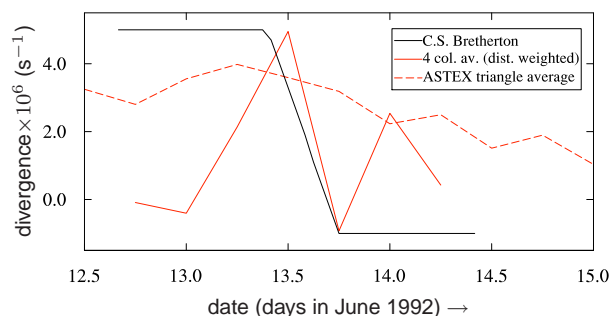

FIG. 3: The large-scale divergence rate as a function of time (June 1992). The solid black line is obtained from ERA-40 and changes sign halfway the First Lagrangian. The red lines show results from ERA-Interim. The solid red line is calculated from a weighted average of divergence rates from the four columns closest to the position of the aircraft, and the dashed red line shows the running mean of the area average divergence rate for the ASTEX triangle.

The determination of the large-scale divergence is difficult. Fig. 3 shows that the results from ERA-Interim are quite different from those found by Bretherton in the ERA-40 data. Ciesielski et al. (1999) used radiosonde observations collected in the ASTEX triangle to calculate the divergence of the horizontal winds. They found $D \approx 5 \times 10^{-6}$ s^{-1}, which is used for the simulation labeled 'div. constant'. Simulations using this constant value caused a too rapid drying and warming of the free atmosphere, after which it was decided to do a second simulation with a time-varying divergence (indicated in the figures by 'div. decreasing') taken from Bretherton et al. (1999b). The geostrophic wind is also changing with time such that the horizontal winds decrease with time in the second half of the Lagrangian in accord with the observations. It should be noted that due to the Lagrangian framework there is no need to prescribe a horizontal advection of heat and moisture.

2.3 *LES domain*

The computational domain for the simulations consists of 128 gridpoints both in the $x-$ and in the $y-$direction, with a resolution of 35 m. A high resolution in the vertical direction is important to properly resolve the strong inversion at the top of the boundary layer. Therefore, a resolution of 15 meters is used inside the boundary layer, while at cloud top it is decreased to 5 meters (following

the case specification by Irina Sandu[4]). In total, 427 levels are used, with the top of the domain at 3050 m. A single simulation of 40 hours, with a dynamic timestep $\leq$1.5 seconds costs about 7000 CPU hours.

2.4 *The Dutch Atmospheric Large-Eddy Simulation (DALES) model*

The simulations were performed using the DALES model, which applies conservation equations for the liquid water potential temperature, total specific humidity and mass for incompressible air. The vertical momentum equation is according to the Boussinesq form with a constant reference density (Heus et al., 2010). Radiation is calculated with the code discussed by Pincus and Stevens (2009), while the microphysics scheme of Khairoutdinov and Kogan (2000), which is based on ASTEX Flight A209 data, is used to calculate drizzle and cloud droplet sedimentation. The surface fluxes are computed from Monin-Obukhov similarity theory.

3. RESULTS

Two large eddy simulations were done, the first of which used a constant divergence $D = 5 \times 10^{-6}$ s^{-1}, while the second used the divergence as was originally prescribed by Chris Bretherton (see Fig. 3). The results of both simulations are discussed in this section. During the first 9 hours, the simulations are identical. The second run is therefore started at 9 UTC using the 3D output fields from the first run for initialization.
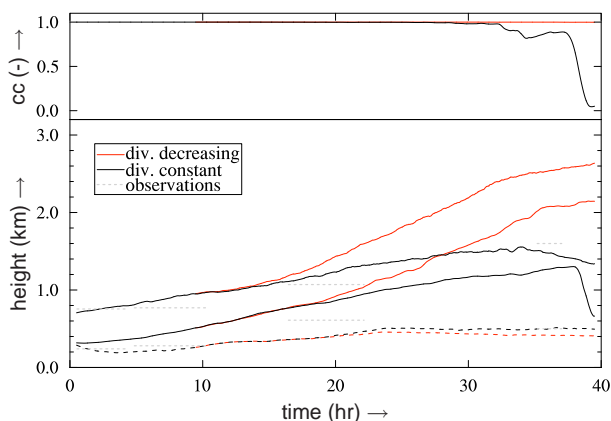
3.1 *Mean state*

FIG. 4: Time series of the domain averaged cloud cover (top) and the cloud top and base (bottom) for the two simulations mentioned in the text. The dotted lines show height of the lowest cloudy gridbox in the domain. A 1-h running mean filter was applied to reduce fluctuations. The dotted grey lines denote the average observed cloud contours during the 2nd to 5th ASTEX flights.

---

[3]http://www.atmos.washington.edu/~breth/astex/lagr/README.hourly.html

[4]http://www.mpimet.mpg.de/en/mitarbeiter/irina-sandu/transition-cases.html

Fig. 4 clearly shows the strong influence of the divergence on the evolution of the stratocumulus layer. After approximately 15 hours, the simulations start to diverge significantly, which eventually results in a large difference in cloud cover. The stratocumulus cloud layer in the constant divergence simulation dissolves completely, causing a rapid drop in cloud cover. The domain-averaged cloud base height also drops rapidly to values close to the minimum cloud base height, which indicates that the only clouds left are cumulus clouds. Because not all of these cumuli extent all the way up to the inversion, the average cloud top also decreases slightly. Interestingly, the height of the boundary layer does not have much influence on the minimum cloud base height, which is about the same for both simulations and does not change much with time.

The subsidence rate $\overline{w}$ is determined by the large-scale divergence rate, $\overline{w} = -Dz$, and the tendency of the boundary layer depth z_i is controlled by an imbalance between the subsidence and entrainment rates,

$$\frac{\mathrm{d}z_i}{\mathrm{d}t} = w_e - z_i D(z_i). \tag{1}$$

Thus a rapid deepening of the boundary layer can be explained by a decreasing divergence rate. After 40 hours, the boundary layer height difference between the simulations is more than 1000 meters. However it should be noted that this is also partly due to different entrainment rates (see Fig. 5). Because the entrainment rate is controlled by the inversion stability, different advective tendencies of heat and moisture in the free atmosphere result in different entrainment rates.

Fig. 6 shows hourly averaged profiles of the liquid water potential temperature θ_L. In the free atmosphere, the warming effect caused by subsidence stops in the simulation with the weakening divergence. The temperature inside the boundary layer, which is mostly controlled by the sea surface temperature, is approximately the same for the two simulations. That means that the θ_L-jump in the second simulation is smaller than that of the one with the constant divergence rate. Subsidence also causes a decrease of q_T in the free atmosphere by advecting dryer air downwards. The simulation with the constant divergence rate exhibits the smallest entrainment rate.

For the simulation in which the subsidence changes sign the free atmospheric air that is entrained into the boundary layer is less dry and therefore, the boundary layer does not dry out as much. This effect is clearly visible in the hour averaged profiles of q_T, shown in Fig. 7, where most of the boundary layer in the second simulation (red line) is more moist than in the first, even though the inversion is much higher.

Figs. 6 and 7 also contain measurements taken during these hours on four of the ASTEX flights. The simulations agree very well with the measurements, especially in the first part of the simulation (hours 3 and 8). After 20 hours of simulation, the effect of the different choices for the divergence becomes clear in the free atmosphere and although the differences are small, the time depen-
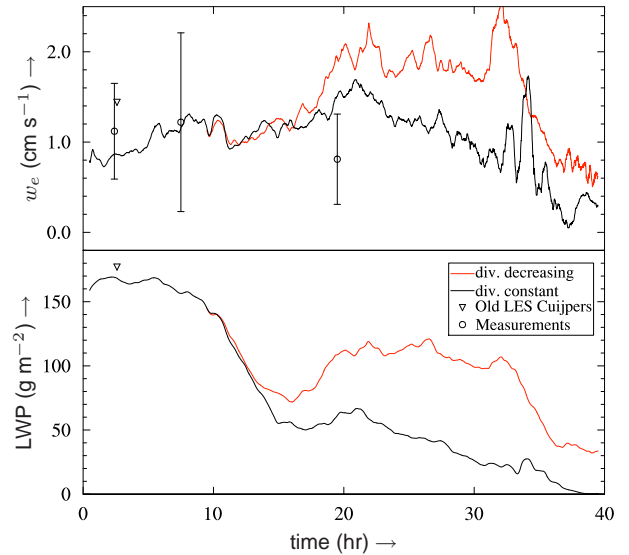

FIG. 5: Time series (1-h running mean) of the domain averaged entrainment rate w_e (top) and the liquid water path LWP (bottom). Also shown are the observed entrainment rates, and results from Hans Cuijpers that he obtained from a LES of the first three hours of the ASTEX Lagrangian as part of the GCSS ASTEX A209 modeling intercomparison study. The entrainment rates were diagnosed from Eq. (1)

dent divergence seems to fit the measurements better. The strong subsidence of the first simulation dries out the air above the boundary layer unrealistically fast. Since subsidence is the only process that influences q_T in the free atmosphere (in the absence of horizontal advection), the decreasing divergence seems to be more in accord with the measurements.

However, from both of the figures mentioned above, it is clear that, of both runs, the inversion height in the constant divergence run is closest to the observations. This is also the general picture when comparing the cloud base and top heights with the observations in Fig. 4. This could suggest that the entrainment rate in the model is too high. This can be verified by comparing future results from other LES models that will be collected as part of the GCSS/EUCLIPSE modeling intercomparison study. Another possible reason could be the presence of some high clouds during the Lagrangian experiment, which act to diminish the longwave radiative cooling at the cloud top. A smaller cooling rate lead to smaller entrainment rates.

The difference in cloud thickness is also reflected in the timeseries of the liquid water path (LWP) of both simulations, which are shown in Fig. 5. During the first day, the LWP drops quite fast, and in the constant divergence case, it keeps diminishing even during the night, to approximately zero at the end of the simulation. The second simulation however, nicely shows a diurnal cycle, with an increase during the night. At the end of this night, the difference between both simulations has reached a max-
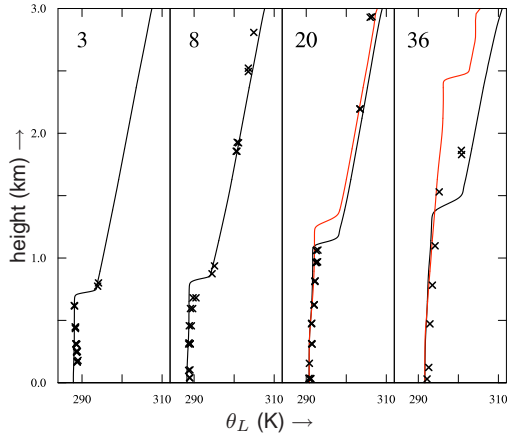
FIG. 6: Hourly averaged vertical profiles of the liquid water potential temperature θ_L of the 3rd, 8th, 20th and 36th hour of the simulations, as well as measurements taken during flights that took place at approximately those hours.

FIG. 7: Hourly averaged vertical profiles of the total water content q_T of the 3rd, 8th, 20th and 36th hour of the simulations, as well as measurements taken during flights that took place at approximately those hours.

imum, about 80 g m^{-2}.

3.2 *Turbulence structure*

The vertical profiles of the turbulent flux $\overline{w'\theta_v'}$ from the LES results, shown in Fig.8, are in a good agreement with the observations. In particular the strong increase in $\overline{w'\theta_v'}$ between the 8th and the 20th hour is well reproduced. During the entire simulation, a part of the buoyancy profile is negative, just below cloud base, both in the measurements and in the simulations, which indicates a tendency towards decoupling of the subcloud from the cloud layer. A negative value for the buoyancy flux effectively acts as a sink for TKE, thereby reducing mixing between subcloud and cloud layer, cutting of most of the moist thermals from the surface. Eventually, this effect also becomes visible in the profiles of the vertical velocity variance, shown in Fig. 9. In particular during the second part of the simulation, these profiles exhibit a distinct maximum in the subcloud and one in the cloud layer. Such a profile indicates that thermals that rise from the sea surface cannot penetrate and transport moisture to the cloud layer. This is an important process explaining thinning of stratocumulus layers.

The profiles of the turbulent kinetic energy (TKE) in Fig. 10 show that the order of magnitude of the turbulent velocity fluctuations in the simulations is similar to that in the observations.

4. CONCLUSIONS

The stratocumulus to cumulus transition as observed during ASTEX is well captured by the large eddy simulation model. A large uncertainty in the large-scale forcing of the simulation is the divergence rate. This divergence relates to the height of the boundary layer directly, while it also affects the stability of the inversion. Therefore, it also influences the entrainment rate and indirectly affects
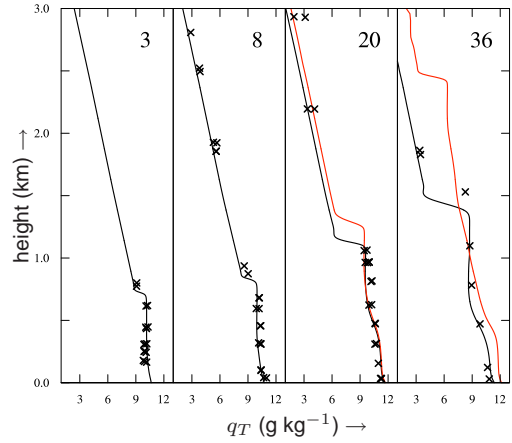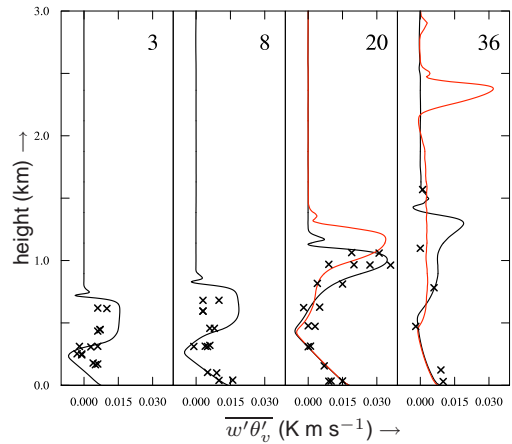

FIG. 8: Hourly averaged vertical profiles of the total virtual potential temperature flux $\overline{w'\theta_v'}$ of the 3rd, 8th, 20th and 36th hour of the simulations, including aircraft measurements.

the evolution of the boundary layer depth. An accurate assessment of the divergence rate is therefore crucial to realistically model the development of the boundary layer. In the near future this case will be run by other LES models and single-column model versions of Earth System Models as part of a new GCSS/EUCLIPSE modeling intercomparison case.
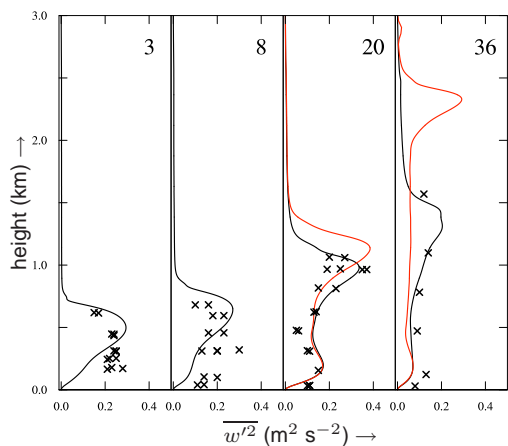
ACKNOWLEDGMENTS

FIG. 9: Hourly-averaged vertical profiles of the resolved vertical velocity variance $\overline{w'^2}$ over the 3rd, 8th, 20th and 36th hour of the simulations, including results from aircraft measurements.
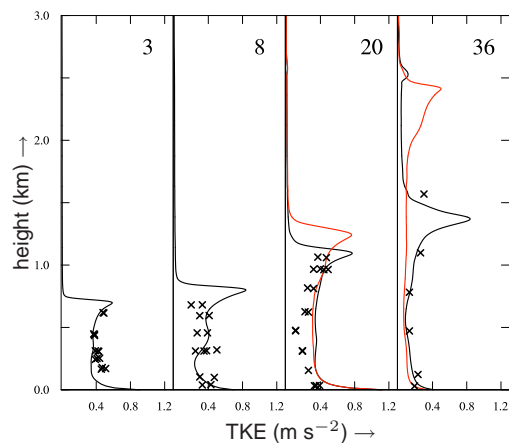

FIG. 10: Hourly averaged vertical profiles of the total turbulent kinetic energy TKE of the 3rd, 8th, 20th and 36th hour of the simulation, including results from aircraft measurements.

REFERENCES

Albrecht, B. A., C. S. Bretherton, D. W. Johnson, W. H. Schubert, and A. S. Frisch, 1995: The Atlantic stratocumulus transition experiment - ASTEX. *Bull. Amer. Meteorol. Soc.*, **76**, 889–904.

Bretherton, C. S., P. Austin, and S. T. Siems, 1995: Cloudiness and marine boundary layer dynamics in the ASTEX Lagrangian experiments. Part II: Cloudiness, drizzle, surface fluxes and entrainment. *J. Atmos. Sci.*, **52**, 2724–2735.

Bretherton, C. S., S. K. Krueger, M. C. Wyant, P. Bechtold, E. V. Meijgaard, B. Stevens, and J. Teixeira, 1999a: A GCSS boundary-layer cloud model intercomparison study of the first ASTEX Lagrangian experiment. *Boundary-Layer Meteorol.*, **93**, 341–380.

Bretherton, C. S., et al., 1999b: An intercomparison of radiatively-driven entrainment and turbulence in a smoke cloud, as simulated by different numerical models. *Quart. J. Roy. Meteorol. Soc.*, **54**, 148–167.

Ciesielski, P. E., W. H. Schubert, and R. H. Johnson, 1999: Large-scale heat and moisture budgets over the ASTEX region. *J. Atmos. Sci.*, **56 (18)**, 3241–3261.

De Roode, S. R. and P. G. Duynkerke, 1996: Dynamics of cumulus rising into stratocumulus as observed during the first "Lagrangian" experiment of ASTEX. *Quart. J. Roy. Meteorol. Soc.*, **122**, 1597–1623.

De Roode, S. R. and P. G. Duynkerke, 1997: Observed Lagrangian transition of stratocumulus into cumulus during ASTEX: Mean state and turbulence structure. *J. Atmos. Sci.*, **54**, 2157–2173.

Duynkerke, P. G., , H.-Q. Zhang, and P. J. Jonker, 1995: Microphysical and turbulent structure of nocturnal stratocumulus as observed during ASTEX. *J. Atmos. Sci.*, **52**, 2763–2777.

Duynkerke, P. G., et al., 1999: Intercomparison of three- and one-dimensional model simulations and aircraft observations of stratocumulus. *Boundary-Layer Meteorol.*, **92**, 453–487.

Duynkerke, P. G., et al., 2004: Observations and numerical simulations of the diurnal cycle of the EUROCS stratocumulus case. *Quart. J. Roy. Meteorol. Soc.*, **130**, 3269–3296.

Heus, T., et al., 2010: Formulation of and numerical studies with the dutch atmospheric large-eddy simulation (DALES). *Geosci. Model Development Discussions*, **3**, 99–180.

Khairoutdinov, M. K. and Y. Kogan, 2000: A new cloud physics parameterization in a large-eddy simulation model of marine stratocumulus. *J. Atmos. Sci.*, **128**, 229–243.

Pincus, R. and B. Stevens, 2009: Monte carlo spectral integration: a consistent approximation for radiative transfer in large eddy simulations. *Journal of Advances in Modeling Earth Systems*, **1**, doi:10.3894/JAMES.2009.1.1.

Sandu, I. and B. Stevens, 2010: On the factors modulating the stratocumulus to cumulus transitions. *J. Atm. Sci., submitted*.

Sandu, I., B. Stevens, and R. Pincus, 2010: On the transitions in marine boundary layer cloudiness. *Atmos. Chem. Phys.*, **10**, 2377–2391.

Seifert, A. and K. D. Beheng, 2001: A double-moment parameterization for simulating autoconversion, accretion and selfcollection. *Atm. Res.*, **118**, 265–281–290, doi:10.1016/S0169-8095(01)00126-0.

Stevens, B., et al., 2005: Evaluation of large-eddy simulations via observations of nocturnal marine stratocumulus. *Mon. Weather Rev.*, **133**, 1443–1462.

Van der Dussen, J. J., 2001: Large eddy and mixed-layer model simulations of the stratocumulus to cumulus transition as observed during astex. M.S. thesis, Delf University of Technology, Utrecht, 72 pp (Available as pdf file from http://www.srderoode.nl/Students/MasterThesisJohan.pdf).